Characterization of Excess Electrons in Water Cluster Anions via Quantum Simulations

László Turi,[1] Wen-Shyan Sheu,[2] and Peter J. Rossky[3]

[1]Eötvös Loránd University, Department of Physical Chemistry, Budapest 112, P. O. Box 32, H-1518, Hungary

[2]Department of Chemistry, Fu-Jen Catholic University, Taipei , Taiwan 242, ROC

[3]Department of Chemistry and Biochemistry, Institute for Theoretical Chemistry, University of Texas at Austin, Austin, TX 78712-1167

Abstract

Water cluster anions can serve as a bridge to understand the transition from gaseous species to the bulk hydrated electron. However, debate continues regarding how the excess electron is bound in $(H_2O)_n^-$, as an interior, bulk-like, or surface electronic state. To address the uncertainty, the properties of $(H_2O)_n^-$ clusters with 20 to 200 water molecules have been evaluated by mixed quantum-classical simulations. The theory reproduces every observed energetic, spectral, and structural trend with *n* that is seen in experimental photoelectron and optical absorption spectra. More importantly, surface states and interior states each manifest a unique signature in the simulation data. The results strongly support assignment of surface bound electronic states to the water cluster anions in published experimental studies thus far.

Clusters are widely studied, both for their direct role in atmospheric and interstellar chemistry, and for their intermediacy between gaseous and condensed phases, which renders them useful simplifying models for complex molecular processes in solution. Negatively charged water clusters have long been used as models to understand the hydrated electron in bulk water. Since its discovery in 1962 (*1*), the hydrated electron has been the subject of numerous experimental (*2-5*) and theoretical studies (*6-10*) for its wide-ranging role in chemical and biological electron transfer. A consistent physical picture of its structural, spectral and dynamic properties has emerged, bolstered in part by details extracted from clusters (*11-26*). However, a key issue remaining with regard to the cluster data is whether the electron is trapped bulk-like, in the cluster interior by oriented solvent molecules, or whether it is stabilized in a surface-bound state, unique to the cluster environment. This issue bears critically on the relation of cluster observations to bulk properties, and the transition from one regime to the other.

Here, we address the question via mixed quantum-classical molecular simulation which allows the direct computation of the experimental observables for these clusters. We show that the available experimental energetic and spectral data are completely consistent with the conclusion that the anionic water clusters observed to date bind the excess electron on the surface, although the long anticipated spontaneous transition to interior states is indicated for clusters in the range of 100-200 molecules.

Barnett *et al.* first identified surface states via a series of quantum mechanical simulations of negatively charged water clusters (*11*). For their model, they found that clusters comprising approximately 8 to 32 water molecules bind the excess electron preferentially in a localized state on the cluster surface. The calculations predicted transition to compact hydrated electron-like interior states with increasing cluster size ($32 < n < 64$). These observations parallel the later

theoretical discovery by Berkowitz and coworkers (*27*) that polarizable atomic anions preferentially adopt surface states in clusters as well (*27-29*).

Experiments have provided indirect insight into the electronic structure. The comprehensive studies of photoelectron spectra in cluster size-selected molecular beams by Coe and Bowen (*15*) led to an excellent correlation of the most probable vertical detachment energy (VDE, the energy needed to remove an electron at the anion's geometry) with the cluster size, n, through the largest cluster measured, $n \leq 69$. For clusters $n \geq 11$, the spectroscopic data fit well to a simple linear relationship in $n^{-1/3}$ for the size dependence based on a dielectric model assuming interior states (*11*). Because the correlation line extrapolated to a value for the infinite cluster that was consistent with simulation of bulk solvated electrons in ambient water, the authors concluded that these clusters were consistent with hydrated electron-like, interior states.

However, in an important theoretical work, Makov and Nitzan developed a continuum dielectric model to evaluate the energy and free energy differences between solvation of a spherical ion (or electron) in the center vs. on the surface of a spherical solvent cluster, and also estimated the VDE's (*13*). For an ion of constant radius in a solvent with high dielectric constant, they showed that the free energy of transfer between the surface and interior of the cluster essentially vanishes. The VDE of a surface state for a negative ion was actually found to be slightly larger than for an ion at the center of the solvent shell. We note that for an electron that is expectedly more delocalized at the surface than in the interior, this difference should be compensated (or possibly overcompensated, thus reversing the VDE ordering). In addition, they showed (*13*) that both interior and surface states manifest the linear scaling of the VDE with $n^{-1/3}$ seen experimentally, so that this scaling did not distinguish the excess electron binding morphologies. Of particular significance, for the infinite cluster, both surface and interior states will therefore extrapolate to the same bulk limit. Hence, the experimental observation of an

extrapolated value close to the bulk does not *a priori* distinguish between surface and interior states.

Later, Ayotte and Johnson (*16*) measured cluster size-selected optical absorption spectra via photodestruction. The spectral peak positions also shift linearly with $n^{-1/3}$, consistent with an excited state energy that also scales with cluster radius. The authors noted that the excited state VDE slope was implicitly smaller than the ground state slope, a result that would be in harmony with different radii for the excited and ground states. The energy gap between the ground and the excited states increased with cluster size, in accord with a contracting radius. They pointed out that of the earlier simulated energies (*11*), those for interior states were quantitatively closer to the measurements than those for surface states. Further, the spectra exhibited not only a blue shift with increasing size, but also an increasing line width. The sequence of spectra appeared qualitatively consistent with a systematic evolution toward the bulk ambient spectrum.

Bartels summarized the entire controversy (*19*) and re-evaluated the optical absorption spectra acquired by Ayotte and Johnson (*16*) based on dispersion relationships. Statistical moment analysis of the spectra yielding values for both the thermally averaged spatial dispersion $\langle r^2 \rangle$, and the kinetic energy $\langle T \rangle$ of the excess electron leads to a distinctive behavior with cluster size: The radius decreases strongly with increasing n, approaching the bulk value from above, while, in parallel, the kinetic energy approaches the bulk value from below. These quantities vary smoothly with n, without the discontinuity in either quantity that might indicate a transition between surface and interior states.

The latest work in the field has come from Neumark and co-workers (*22*) who measured the photoelectron spectra of larger water cluster anions ($n \leq 150$), for clusters generated with both low and high backing pressures, the latter yielding presumably colder clusters. This study raised

the question of temperature dependence directly, although Barnett and co-workers had provided a limited consideration (*11*) and Johnson had noted that cluster temperature is a function of preparation method and cluster size (*16*). We note that the uniform continuum model has only a weak temperature dependence. Neumark's group observed a new feature in the photoelectron spectra in colder clusters, with significantly smaller VDE's than those found by Coe *et al* (*15*). Because of the smaller VDE, they attributed the new peaks to the presence of surface states, and concluded that the earlier work had, therefore, observed interior states.

Here, we report a series of mixed quantum-classical, fully molecular simulations on $(H_2O)_n^-$ clusters with *n*=20, 30, 45, 66, 104 and 200, with internal kinetic energies consistent with three different temperatures 100 K, 200 K and 300 K. The simulation methods are described in more detail elsewhere (*6*, *8*, *10*, *30*). The water molecules are described classically, interacting via a flexible three-site potential, whereas the electron is represented by its wavefunction in a plane-wave basis evenly distributed on a 32×32×32 point grid. The water-electron interaction is modeled by a recent approximate pseudopotential model (*10*). Sampling is done by molecular dynamics. The water molecules evolve under the combined influence of other classical molecules and the electron. The nuclear evolution is adiabatic; the electron remains in its ground state. All the cluster simulations have been initiated from interior states of previous hydrated electron simulations (*10*). The equilibration of the systems has included tests to specifically establish that the surface states result from spontaneous migration from an interior state to the cluster surface state.

In this work, we have not attempted to directly evaluate the relative free energies of surface and interior states. Thus, in the ensuing discussion 'stability' refers simply to the persistence of that state over the duration of the simulation. The data reported here have been obtained from

equilibrated trajectories of 30 to 80 ps length. These durations are approximately an order of magnitude longer than those of Barnett and co-workers (*11*). The present method employs several approximations, including the use of classical nuclei, the neglect of explicit solvent polarizability, and the use of an approximate electron-water pseudopotential which neglects electron solvent dispersion interactions *(23)*. Simulations using the same set of approximations for the bulk hydrated electron give results that are consistent with experiment (*10*). Because these approximations are expected to introduce significant quantitative error for smaller clusters *(23)*, we consider only $n \geq 20$ here. In particular, the use of the present water model's fixed charge polarization, appropriate to the bulk liquid environment, is likely to overestimate the molecular dipole in a small cluster, and correspondingly artificially enhance the electrostatic electron binding. Spectral results on the hydrated electron at low bulk density and high temperature *(31)* indicate that models like those used here are correspondingly limited in that regime.

The electronic distributions for the ground state anions fall in two distinct categories. Identification follows from the radius of the cluster (r_c), the electron radius (radius of gyration, $r_e = \left\langle r^2 \right\rangle^{1/2}$), and the distance between the centers of the electron and water distributions (R). An interior state is localized within the cluster, so that $R + r_e < r_c$. For a surface state, $R \sim r_c$, and significant electronic amplitude appears outside the nominal cluster radius (Fig. 1). It is notable that the surface electronic states are highly analogous to bulk hydrated electron distributions (*6*), with typical *s* and *p* character. At 200 and 300 K, we find that only the $n = 200$ cluster exhibits a stable interior electronic state; all smaller clusters ($n = 20$, 30, 45, 66 and 104) support stable surface states. At 100 K, only the smallest clusters, up to $n = 45$, spontaneously manifest the excess electron on the surface. Larger clusters, and an alternative $n = 45$ configuration, are stable

with the electron in an interior state. However, this may be a kinetic effect, and we cannot conclude from this that the lower temperature favors interior states.

The validity of these calculations can be tested via the computed physical properties of the clusters such as absorption spectra at different temperatures (Fig. 2). The spectral evolution of the surface state clusters, in terms of both shift and width, completely parallels the experimental spectra of Ayotte and Johnson (*16*). There is only weak temperature dependence for surface states. The experimental spectral trends should therefore be substantially the same over a very wide range of cluster temperatures, as long as the electron is surface bound.

In contrast, the spectrum at 300 K for the n = 200 interior state, is nearly identical to the bulk hydrated electron spectrum (*10*). At 200 K, the corresponding n=200 spectrum is slightly blue-shifted from the bulk peak center at 298 K (*10*). At 100 K, the spectral evolution exhibits a sharp shift at the point of surface to interior transition (at $n \approx 45$), and at n = 200 is blue-shifted by nearly 0.5 eV from the bulk simulated spectrum at 298 K (*10*). This characteristic blue-shift from the bulk spectrum would be an experimental signature of cold interior states. We attribute the temperature dependence of the interior state clusters to solvent contraction (electrostriction) around the electron with decreasing temperature. For surface states, a contraction of solvent does not increase confinement of the electron. For the bulk hydrated electron, simulations (*32*) with the same model used here (*10*) have qualitatively reproduced the experimental temperature dependence of spectra in the liquid and shown that at liquid densities, this dependence lies predominantly, although not entirely *(31)* in the solvent density response.

The temperature dependence observed here contradicts the conclusions in the seminal simulations of Barnett *et al.* (*11,12*); the discrepancy is likely due to the difference in model and/or the limited sampling accessible in the older work. Our low temperature spectra do appear qualitatively similar to those of Barnett *et al.* (*12*) except for the size dependence. As noted, the

surface to interior transition occurred there between n = 32 and 64 at 300 K (*11*), whereas our model predicts a transition in the $104<n<200$ range.

The calculated spectra shown in Fig. 2 broaden and shift to the blue with increasing cluster size, in excellent agreement with experiment. The blue shift results from a sharper increase in stabilization of the *s*-state than of the more diffuse *p*-state as the cluster grows. The broadening is assignable primarily to an increasing *p*-state splitting. For smaller clusters the *p*-states are more nearly degenerate in each configuration, leading to overall narrower spectra.

Extrapolation of the calculated spectral maxima energies and vertical detachment energies to infinite cluster size is compared in Fig. 3 with the extrapolations of analogous experimental data from Coe (*15*) and Johnson (*16*). Because the surface states exhibit only weak temperature dependence, the surface state points in the plot are averaged over the temperatures simulated. The simulated surface state data follow a slope similar to the experiment. Also, as in experiment (*16*), the ground state energy (VDE) slope is different from that for the excited state, and, correspondingly, both lines extrapolate to very near the ambient bulk values for the model. This result is expected based on the continuum dielectric model (*13*). In contrast, the simulated interior state data clearly differ from experiment, and the low temperature data do not extrapolate to room temperature bulk properties. If the surface to interior state transition does occur above n=104, we find that the observed results of Coe (*15*) and Johnson (*16*) would then be consistent with our simulated results over a wide range of actual cluster temperatures.

Comparison of the calculated radius of gyration and kinetic energy data with experiment makes an even more compelling case than the spectral data for predominance of surface states (Fig. 4). The distinct trends with cluster size follow the experimentally derived size dependence (*19*) faithfully (cf. Figure 1 of Reference 19). The radius smoothly approaches the bulk value from above as the clusters grow, whereas the interior states have nearly identical radii. A similar

pattern holds for the kinetic energy; the trend follows experimentally derived size dependence (*19*). The interior states have much higher kinetic energy than the surface states. There is some increase with decreasing temperature, but all interior state kinetic energies are similar to the large cluster limit. These trends are qualitatively similar to those seen originally by Barnett (*11*), though different in magnitude.

Some additional insight into the regularity of the behavior of the surface state clusters can be obtained by computing the mean dipole polarization $<\mu>$ of the molecular clusters in the direction of the electronic center of charge. The surface states manifest a variation of $<\mu>$ in the 15 to 33 Debye range, for $20 < n < 104$ cluster sizes at 200K, with a nearly linear dependence on $n^{-1/3}$, in accord with the expected size dependence of the Makov-Nitzan dielectric model (*13*). This molecular cluster dipole moment largely compensates the dipole associated with the position of the surface bound electron with respect to the cluster center of mass.

There are quantitative shortcomings in the calculated values compared to experimental reports. The calculated VDE values are closer to those only recently measured by Neumark *(22)* for the identified surface states (denoted there as Isomer II) than to the Coe data (15) considered here. However, the surface and interior electron binding morphologies lead to distinctly different trends in measured physical properties: vertical detachment energy, optical absorption spectra, kinetic energy and electronic radius. The comparison of the trends to the corresponding published experimental data strongly supports the conclusion that the available experiments reporting these results reflect only clusters characterized by electronic surface states. The newly reported species associated with more weakly bound electrons (*22*) are presumably also surface states, as concluded in that report, but they do not appear to be a simple extrapolation of those found here. We have carried out a set of preliminary simulations that show that electrons attached to already

formed very cold water clusters produce surface state species with a range of vertical electronic detachment energies of magnitudes well below those of the clusters simulated here. We therefore speculate that the surface states recently observed are the result of such attachment processes. The differences may reflect alternative proton ordering motifs, as suggested by Johnson and coworkers *(25,26)*.

Our findings substantially support the physical picture originally put forth by Barnett and co-workers (*11*) and strongly suggest that for larger clusters than observed to date, the transition to an interior state should occur. Most importantly, the results indicate that both the physical state and cluster temperature of interior states can be characterized from optical spectra, or from the character of the high-energy end (VDE > 3.0 eV) of photoelectron spectra.

These results reinforce the conclusion that simple continuum dielectric models of these clusters have considerable power, particularly for surface states, but are limiting in describing the temperature dependence of the spectra and kinetic energy, key factors in the interpretation of data for interior states. The weak temperature sensitivity of surface states clearly explains why extrapolation of the surface state properties leads to a value close to the bulk ambient VDE, as this bulk state is nearly isoenergetic with the actual extrapolation limit, the semi-infinite solvent surface state (*13*). The relatively large temperature dependence of interior state properties also emerges as a convenient way to distinguish the two binding morphologies. Finally, we note that nuclear quantum effects on water structure will play a role in the quantitative comparison of experiment and simulations. Classical water clusters are expected to exhibit the characteristics of significantly colder systems when considered at the same nominal temperature as experimental (quantized) water clusters (*8*, *33*).

References

1. E. J. Hart and J. W. Boag, *J. Am. Chem. Soc*. **84**, 4090 (1962).

2. A. Migus, Y. Gauduel, J. L. Martin and A. Antonetti, *Phys. Rev. Lett.* **58**, 1559 (1987).

3. F. H. Long, H. Lu and K. B. Eisenthal, *Phys. Rev. Lett.* **64**, 1469 (1990).

4. C. Silva, P. K. Walhout, K. Yokoyama, and P. F. Barbara, *Phys. Rev. Lett.* **80**, 1086 (1998).

5. M. J. Tauber, and R. A. Mathies, *J. Am. Chem. Soc.* **125**, 1394 (2003).

6. P. J. Rossky and J. Schnitker, *J. Phys. Chem.* **92**, 4277 (1988).

7. A. Wallqvist, G. Martyna and B. J. Berne, *J. Phys. Chem.* **92**, 1721 (1988).

8. B. J. Schwartz and P. J. Rossky, *J. Chem. Phys.* **101**, 6902 (1994)

9. A. Staib and D. Borgis, *J. Chem. Phys.* **103**, 2642 (1995).

10. L. Turi and D. Borgis, *J. Chem. Phys.* **117**, 6186 (2002).

11. R. N. Barnett, U. Landman, C. L. Cleveland, and J. Jortner *J. Chem. Phys.* **88**, 4429 (1988).

12. R. N. Barnett, U. Landman, G. Makov, and A. Nitzan *J. Chem. Phys.* **93**, 6226 (1990).

13. G. Makov and A. Nitzan, *J. Phys. Chem.* **98**, 3459 (1994).

14. H. Haberland, H. G. Schindler and D. R. Worsnop, *Ber. Bunsenges. Phys. Chem.* **88**, 270 (1984).

15. J. V. Coe, G. H. Lee, J. G. Eaton, S. T. Arnold, H. W. Sarkas, K. H. Bowen, C. Ludewigt, H. Haberland and D. R. Worsnop *J. Chem. Phys.* **92**, 3980 (1990).

16. P. Ayotte and M. A. Johnson, *J. Chem. Phys.* **10**6, 811 (1997).

17. P. Ayotte, G. H. Weedle, C. G. Bailey, M. A. Johnson, F. Vila and K. D. Jordan *J. Chem. Phys.* **110**, 6268 (1999).

18. J. V.Coe, *Int. Rev. Phys. Chem.* **20**, 33 (2001).

19. D. M. Bartels, *J. Chem. Phys.* **115**, 4404 (2001).

20. A. E. Bragg, J. R. R. Verlet, A. Kammrath, O. Cheshnovsky, and D. M. Neumark, *Science*, **306**, 669 (2004).

21. D. H. Paik, I-R. Lee, D.-S. Yang, J. S. Baskin, and A. H. Zewail, *Science*, **306**, 672 (2004).

22. J. R. R. Verlet, A. E. Bragg, A. Kammrath, O. Cheshnovsky, and D. M. Neumark, *Science*, **307**, 93 (2005).

23. F. Wang, K. D. Jordan, *Ann. Rev. Phys. Chem.*, **54**, 367 (2003).

24. K. D. Jordan, *Science* **306**, 618 (2004).

25. N. I. Hammer, J.-W. Shin, J. M. Headrick, E. G. Diken, J. R. Roscioli, G. H. Weddle, M. A. Johnson, *Science*, **306**, 675 (2004).

26. N. I. Hammer, J. R. Roscioli, M. A. Johnson, *J. Phys. Chem. A* (in press).

27. L. S. Sremaniak, L. Perera, and M. L. Berkowitz, *J. Phys. Chem.* **100**, 1350 (1996).

28. G. H. Peslherbe, B. M. Ladanyi, and J. T. Hynes, *Chem. Phys.* **258**, 201 (2000).

29. P. Jungwirth, and D. J. Tobias, *J. Phys. Chem. B* **106**, 6361 (2002).

30. F. A. Webster, P. J. Rossky and R. A. Friesner, *Comput. Phys. Commun.* **63**, 494 (1991).

31. D. M. Bartels, K. Takahashi, J. A. Cline, T. W. Marin, C. D. Jonah, *J. Phys. Chem. A* **109**, 1299 (2005).

32. C. Nicolas, A. Boutin, B. Lévy and D. Borgis, *J. Chem. Phys.* **118**, 9689 (2003).

33. H.Gai, G. K. Schenter, L. X. Dang, and B. C. Garrett, *J. Chem. Phys.* **105**, 8835 (1996).

34. This work was supported by research grants to LT from the Bolyai Research Fellowship, the Foundation for Hungarian Higher Education and Research, Ministry of Education, Hungary (0140/2001), and from the National Research Fund of Hungary (OTKA, T049715); by a grant to PJR from the US National Science Foundation (CHE 0134775) and by the R. A. Welch Foundation (F-0019); and by a grant to WSS from the National Science Council, ROC (Contract No. NSC 93-2113-M-030-006). We thank Dr. Carlos Lopez for his assistance in preparing Fig. 1.

Figure Captions

Figure 1. Typical electronic distributions for the surface state of $(H_2O)_{45}^-$. Left: Ground state, isosurface enclosing 80% of electron density, with inner shadow isosurface at 30%; Right: Excited state, isosurface enclosing 80% of electron density.

Figure 2. Optical absorption spectra for $(H_2O)_n^-$ clusters at kinetic energies characteristic of three different temperatures, 300 K, 200 K and 100 K, respectively. The first three sub-bands of each spectrum are also indicated (curves within envelope). The arrows at the bottom indicate the simulated bulk hydrated electron spectral maximum for the same model at 298 K (*10*). The trend with *n* of surface state spectra follows that observed in the experimental spectra (see Figure 2 of (*16*)).

Figure 3. Simulated mean VDE's and spectral maxima for optical absorption for $(H_2O)_n^-$. The surface state data (filled circles) are reported as the average over all temperatures studied. All data for the interior states (open symbols) fall in the highlighted rectangular area. (∇, 100 K; **Δ**, 200 K; □, 300 K). The bold stars at $n^{-1/3} = 0$ indicate the simulated bulk hydrated electron values at 298 K (*10*). The linear fits derived from the VDE data from Coe and Bowen (*15*), and the spectral maxima of Ayotte and Johnson (*16*) are also shown (dashed lines). The vertical dotted lines indicate the maximum experimental cluster sizes reported in (*15*) and (*16*). The linear extrapolation of the simulations is very similar to that seen in experiment. (cf. Figure 3 of (*16*)).

Figure 4. Radius of gyration and kinetic energy of the excess electron in water cluster anions at three simulation temperatures; 100 K (∇), 200 K (**Δ**) and 300 K (□). Filled symbols denote surface states, open symbols denote interior states. The dashed lines show the simulated radius of

gyration and kinetic energy of the hydrated electron in bulk water at 298 K (*10*). The surface state data behave comparably to the experimental data (cf. Figure 1 of (*19*)).

Figure 1.

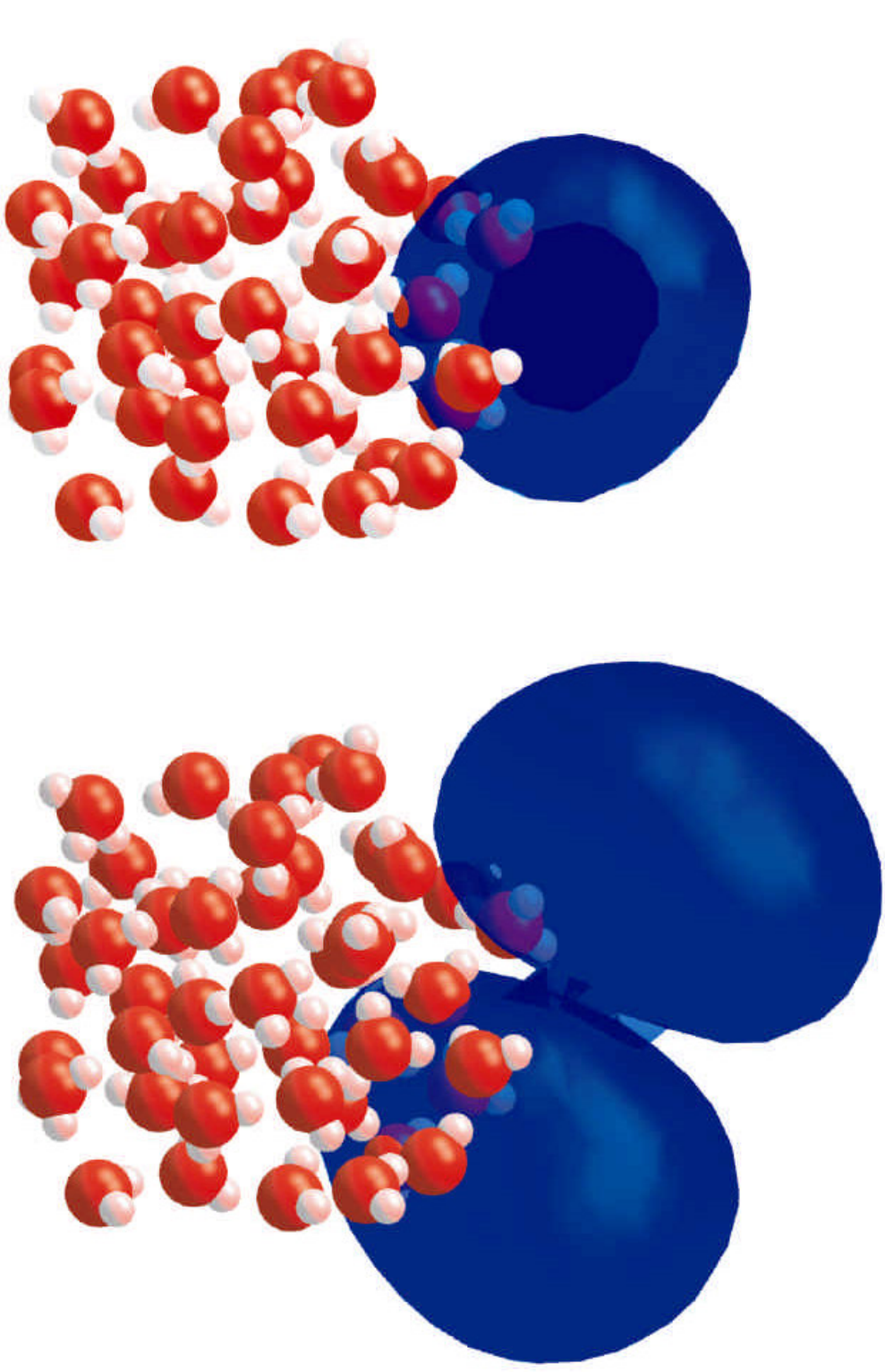

Figure 2.

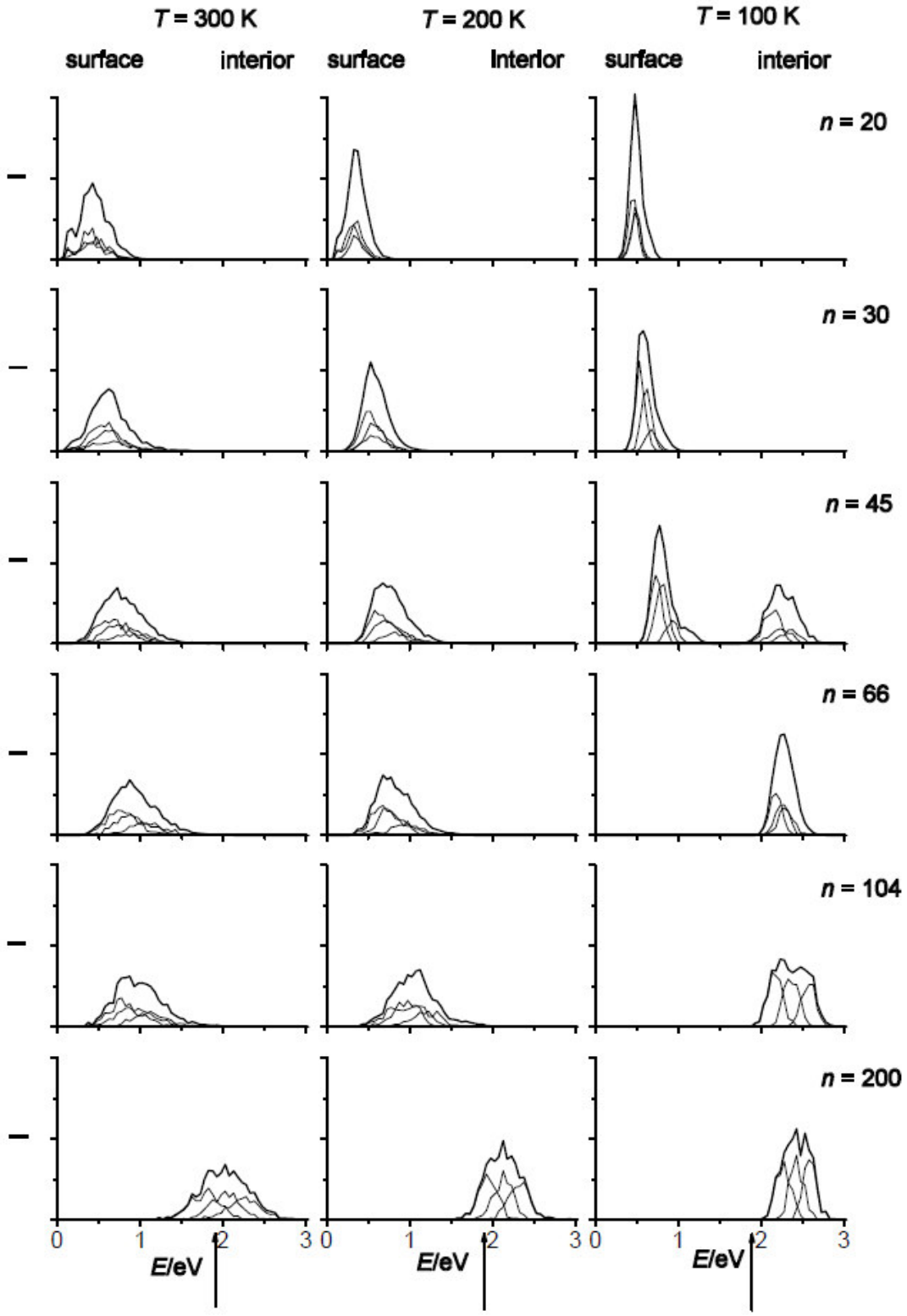
T = 300 K
T = 200 K
T = 100 K
surface
interior
surface
Interior
surface
interior
n = 20
n = 30
n = 45
n = 66
n = 104
n = 200
0
1
2
3
E/eV

Figure 3.

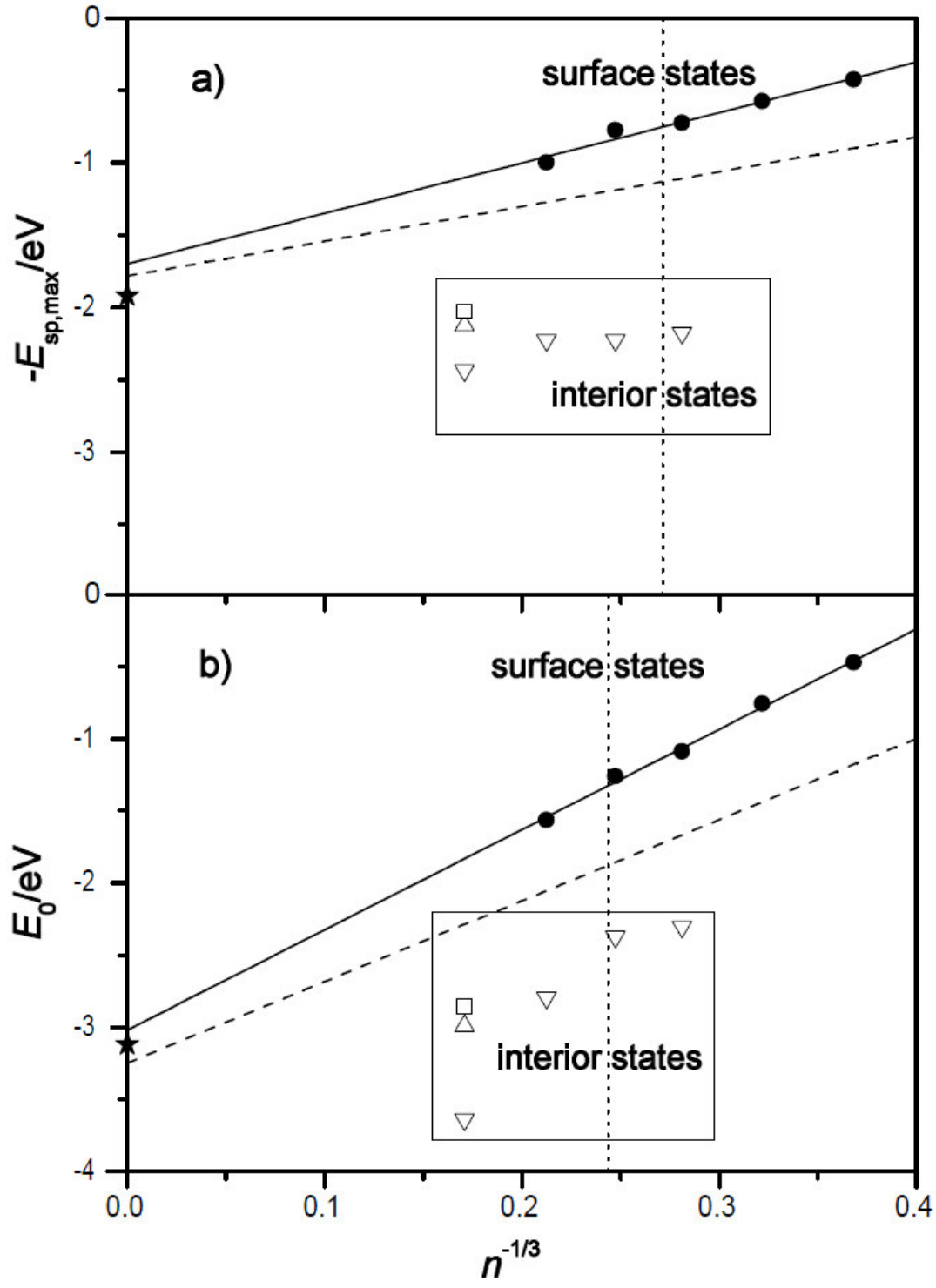
a)
surface states
interior states
$-E_{sp,max}$/eV
b)
surface states
interior states
E_0/eV
$n^{-1/3}$
0
-1
-2
-3
-4
0.0
0.1
0.2
0.3
0.4

Figure 4.

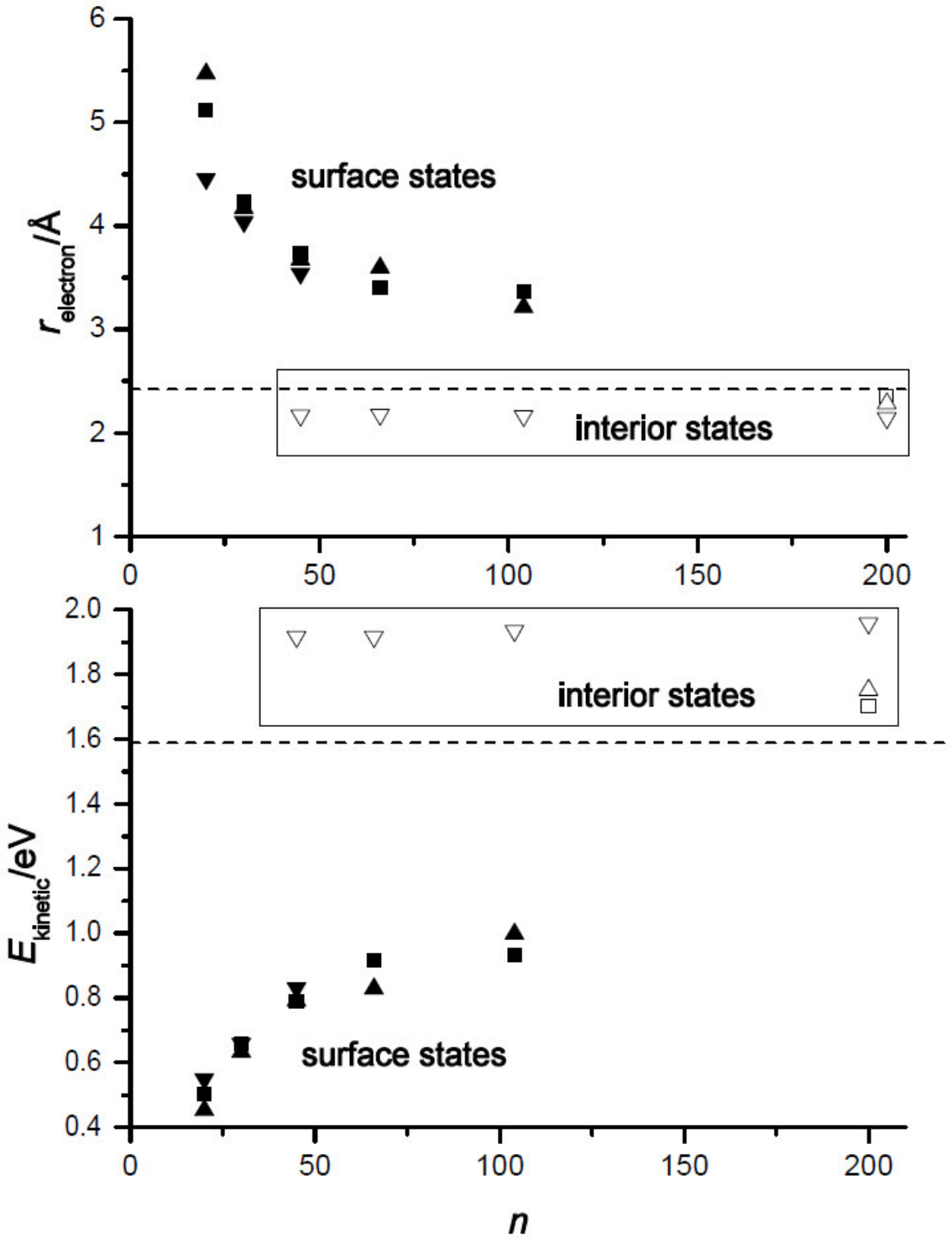
$r_{electron}$/Å
surface states
interior states
$E_{kinetic}$/eV
interior states
surface states
n